Supporting Information

Novel A-π-D-π-A-type BODIPY dyads as small-molecule donor for solution-processed organic solar cells

Bao Xie, [a] Lunxiang Yin [a], Junmei Fan [b], Chang Liu [a] and Yanqin Li *[a]

[a]*School of Chemical Engineering, Dalian University of Technology, Linggong Road 2, Dalian, P. R. China.*

E-mail: liyanqin@dlut.edu.cn; Tel: +86-155-24572530.

[b]*School of Mathematical Sciences, Dalian University of Technology, Linggong Road 2, Dalian, P. R. China.*

Table of Contents

1. Theoretical calculation

The design concept of BODIPY molecules is presented in **Fig. S1**. Density functional theory (DFT) and time-dependent density functional theory (TD-DFT) calculations were conducted by Gaussian 09 software at the B3LYP/6-31G(d) level.[1] The optimized geometries, frontier orbital energy levels, electronic density distributions and the predicted UV-vis absorption spectra of **CBDP**, **DCBDP**, **CTBDP** and **DCTBDP** are shown in **Fig. S2**. The calculated data of electronic transitions for these molecules are also summarized in **Table S1**.

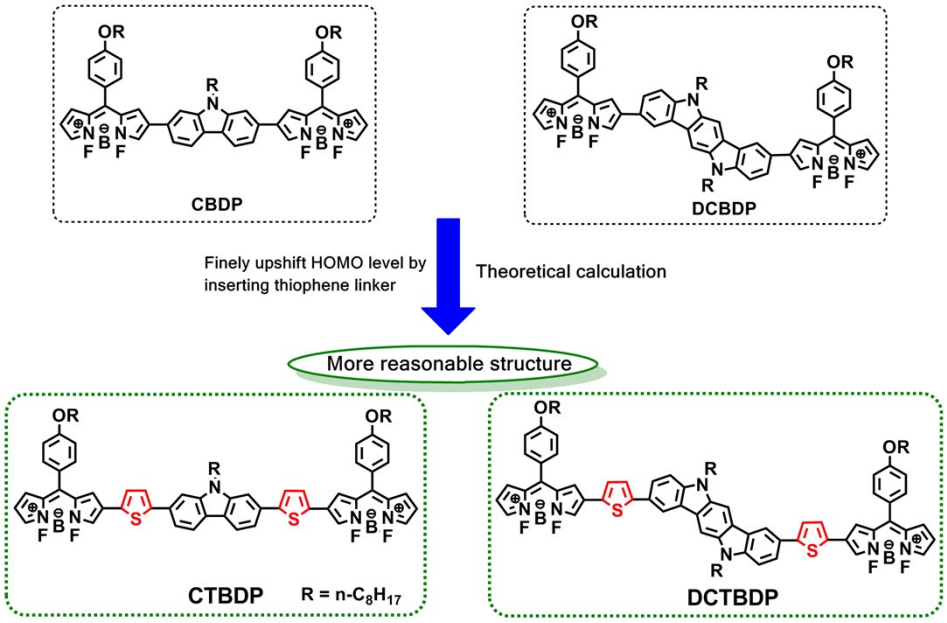

Fig. S1 The design concept of BODIPY molecules with DFT calculation method.

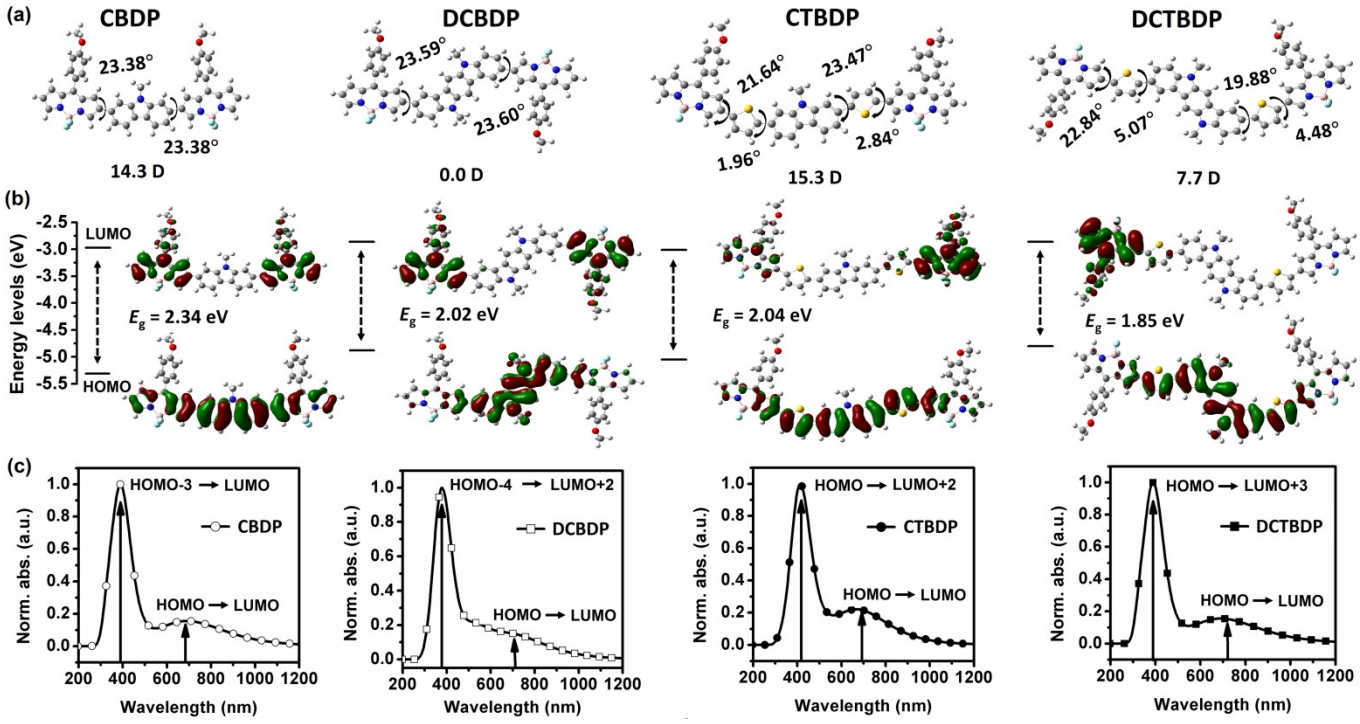

Fig. S2 (a) The optimized geometries; **(b)** energy-level and electronic density distributions; **(c)** predicted UV-vis absorption spectra of **CBDP**, **DCBDP**, **CTBDP** and **DCTBDP** respectively.

Table S1 The energy level, bandgap, dipole moment and total energy of **CBDP**, **DCBDP**, **CTBDP** and **DCTBDP** based on ground-state optimized configurations with DFT calculation.

Molecule	$HOMO^{DFT}$ (eV)	$LUMO^{DFT}$ (eV)	*E*DFT g (eV)	Dipole moment (Debye)	Total energy ($\times 10^6$ kJ mol^{-1})
CBDP	-5.31	-2.97	2.34	14.3	-6.8
DCBDP	-4.88	-2.86	2.02	0.0	-7.7
CTBDP	-5.05	-3.01	2.04	15.3	-9.7
DCTBDP	-4.80	-2.95	1.85	7.7	-10.6

Table S2 The electronic transitions for **CBDP**, **DCBDP**, **CTBDP** and **DCTBDP** with TD-DFT calculation.

Molecule	State	*E* (eV)	λ (nm)	*f*	Composition
CBDP	S1	2.04	609	0.4902	HOMO → LUMO (70%)
	S6	2.82	440	0.2448	HOMO-2 → LUMO+1 (67%)
	S8	3.14	394	0.3891	HOMO-4 → LUMO (52%)
	S9	3.18	390	0.6872	HOMO-3 → LUMO (66%)
	S11	3.41	363	0.2388	HOMO-4 → LUMO+1 (53%)
	S13	3.48	356	0.4499	HOMO-6 → LUMO+1 (56%)
	S20	3.93	315	0.3234	HOMO → LUMO+2 (57%)
DCBDP	S1	1.72	721	0.2265	HOMO → LUMO (70%)
	S5	2.36	526	0.2077	HOMO-1 → LUMO+1 (69%)
	S7	2.96	419	0.2441	HOMO-3 → LUMO (66%)
	S9	3.15	394	0.3378	HOMO-5 → LUMO (48%)
	S11	3.21	386	0.6903	HOMO-4 → LUMO+2 (66%)
	S14	3.43	362	0.3469	HOMO-7 → LUMO (44%)
CTBDP	S1	1.78	695	0.4888	HOMO → LUMO (69%)
	S7	2.90	428	1.6122	HOMO → LUMO+2 (47%)
	S9	3.04	408	0.3071	HOMO-3 → LUMO (40%)
	S10	3.09	401	0.4202	HOMO-5 → LUMO+1 (47%)
	S11	3.12	398	0.5389	HOMO-5 → LUMO (35%)
DCTBDP	S1	1.63	763	0.2614	HOMO → LUMO (66%)
	S9	3.01	412	0.8450	HOMO-4 → LUMO (52%)
	S13	3.11	398	0.2499	HOMO → LUMO+2 (44%)
	S14	3.19	389	1.2934	HOMO → LUMO+3 (43%)
	S27	3.72	334	0.5948	HOMO-1 → LUMO+4 (43%)

2. ^{1}H NMR and ^{13}C NMR spectra

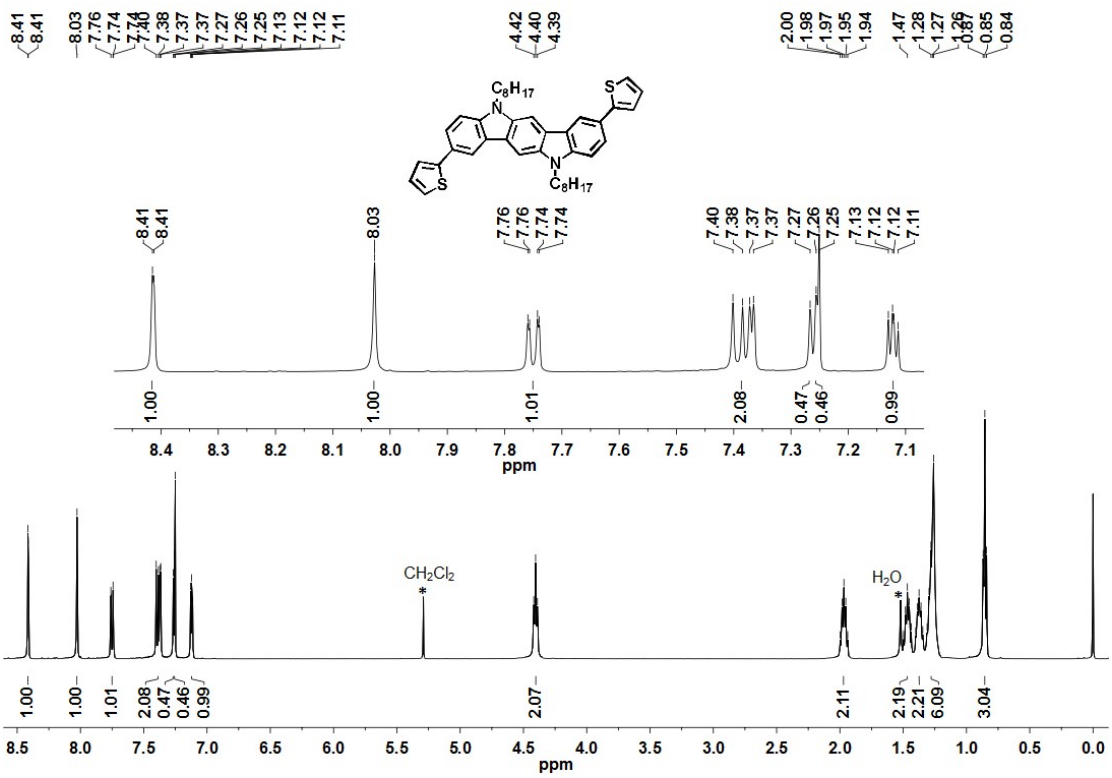

Fig. S3 ^{1}H NMR spectrum of compound 4

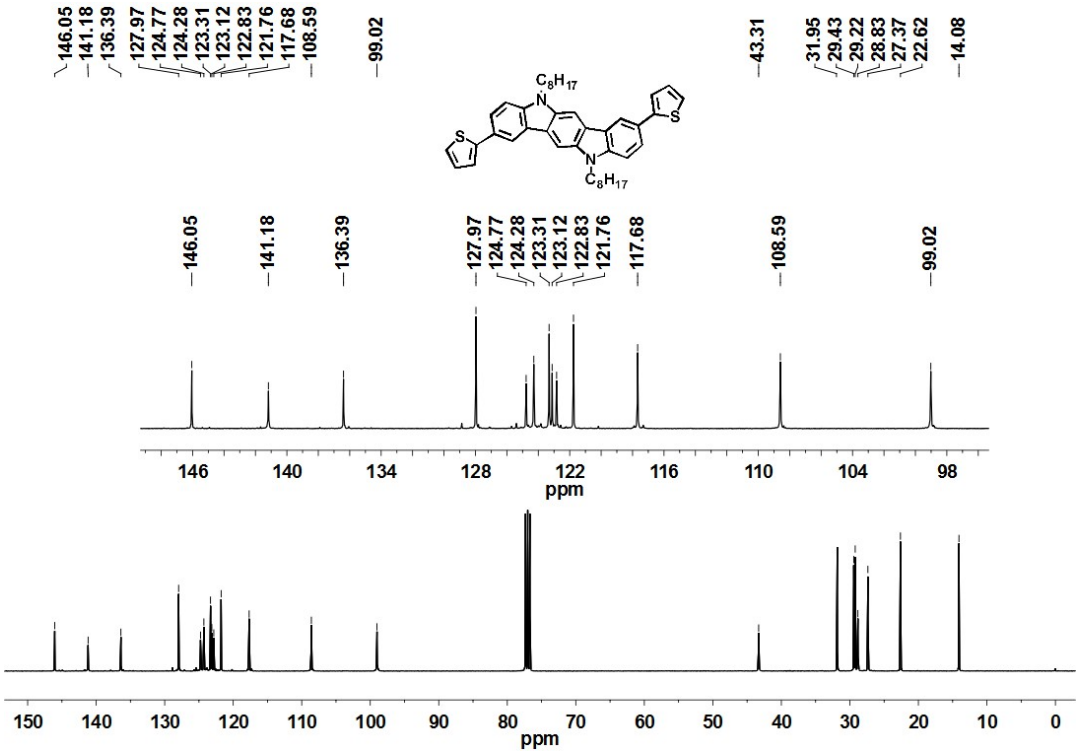

Fig. S4 ^{13}C NMR spectrum of compound 4

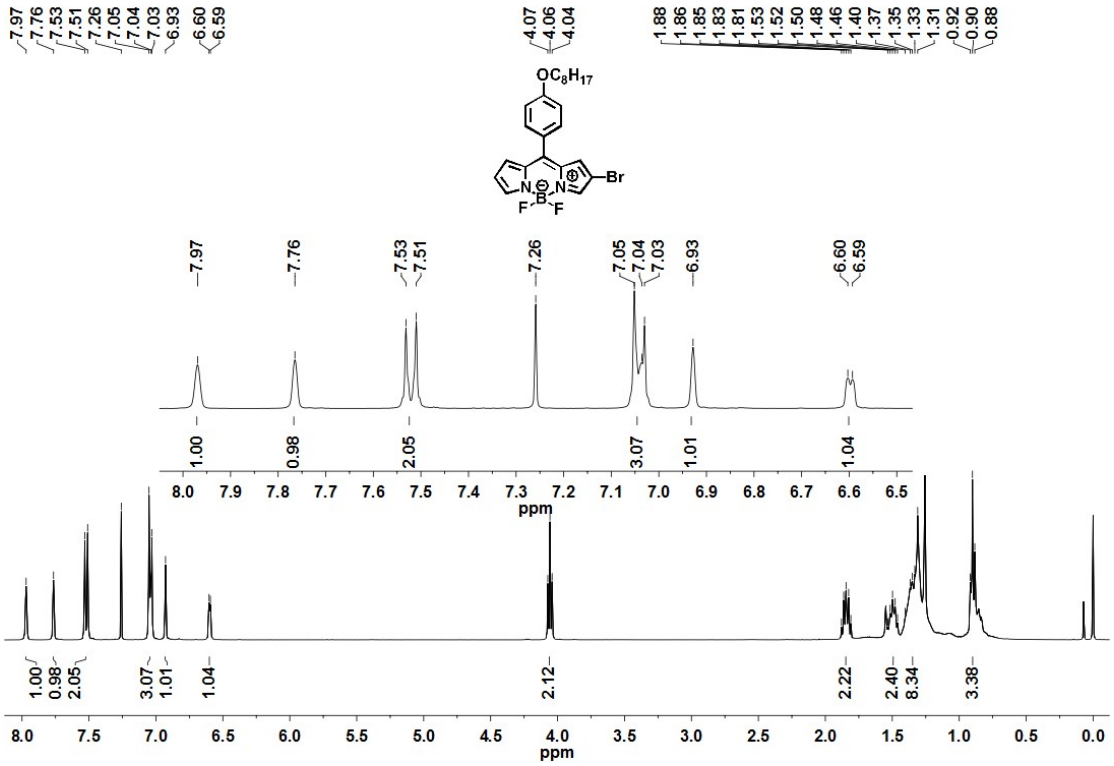

Fig. S5 ^{1}H NMR spectrum of compound 7

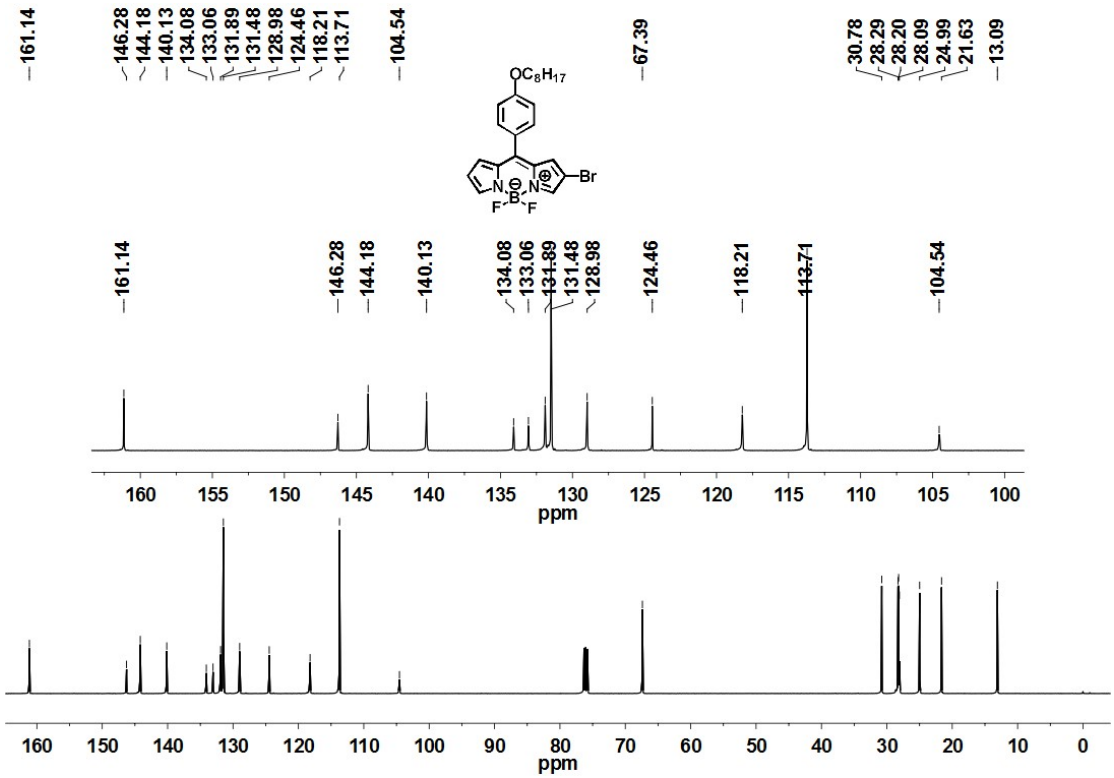

Fig. S6 ^{13}C NMR spectrum of compound 7

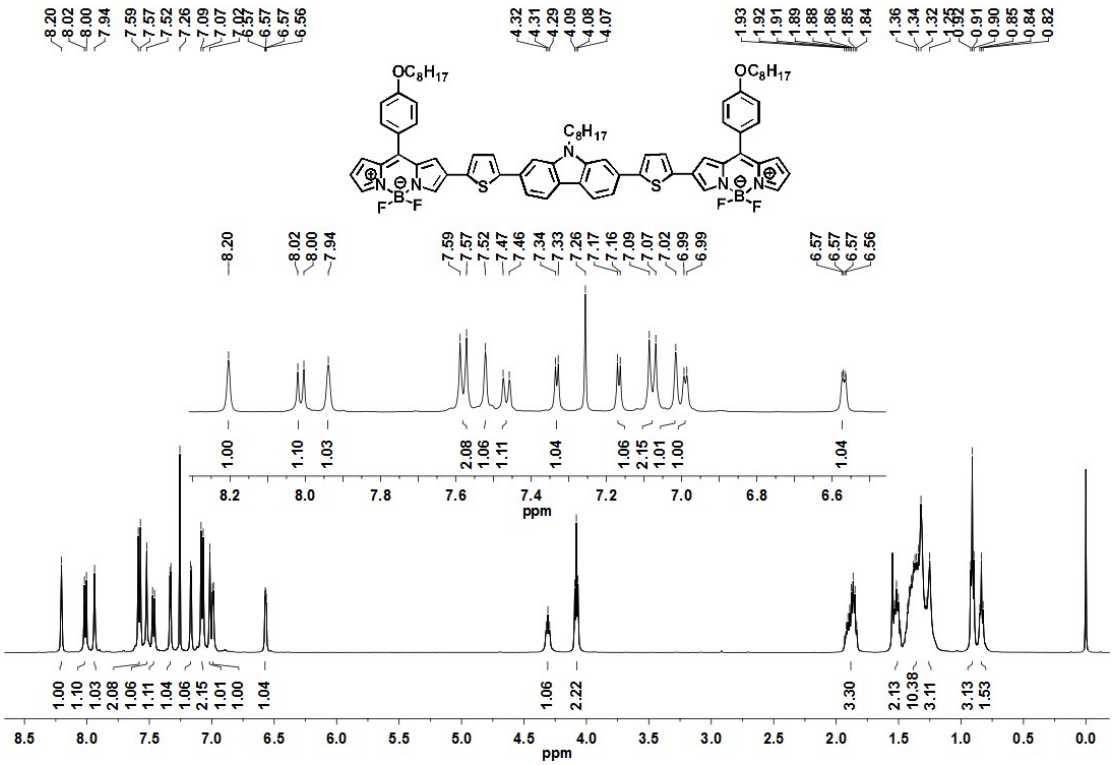

Fig. S7 ^{1}H NMR spectrum of **CTBDP**

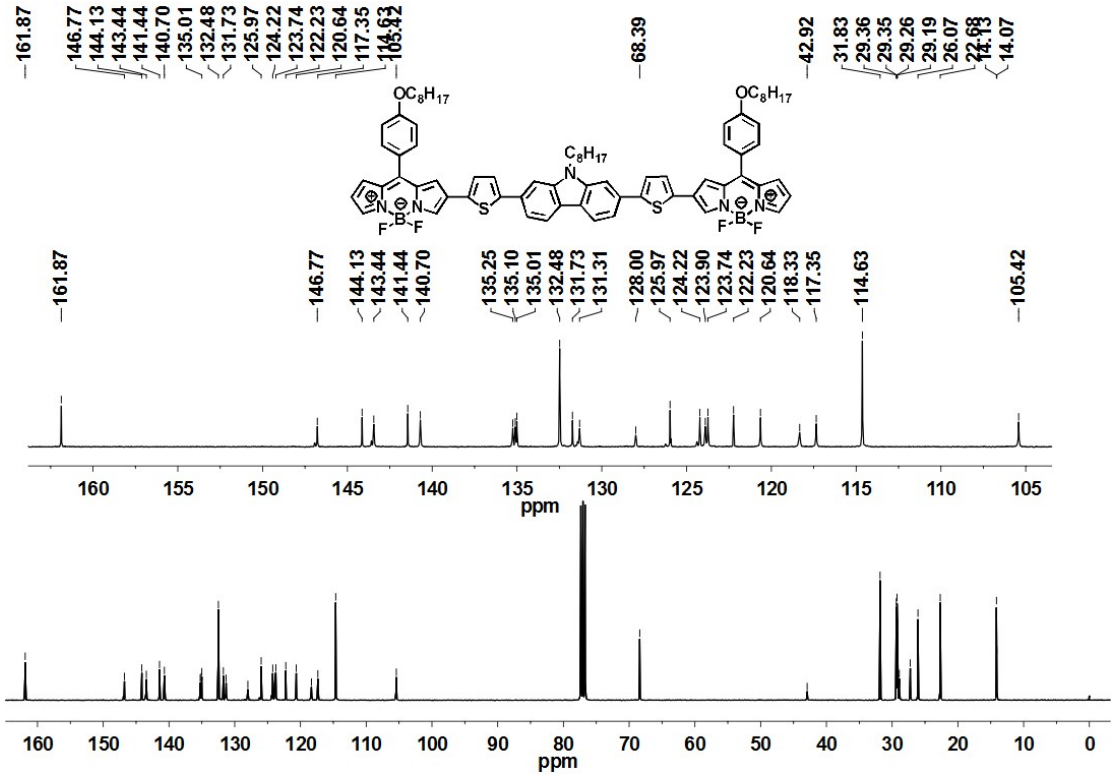

Fig. S8 ^{13}C NMR spectrum of **CTBDP**

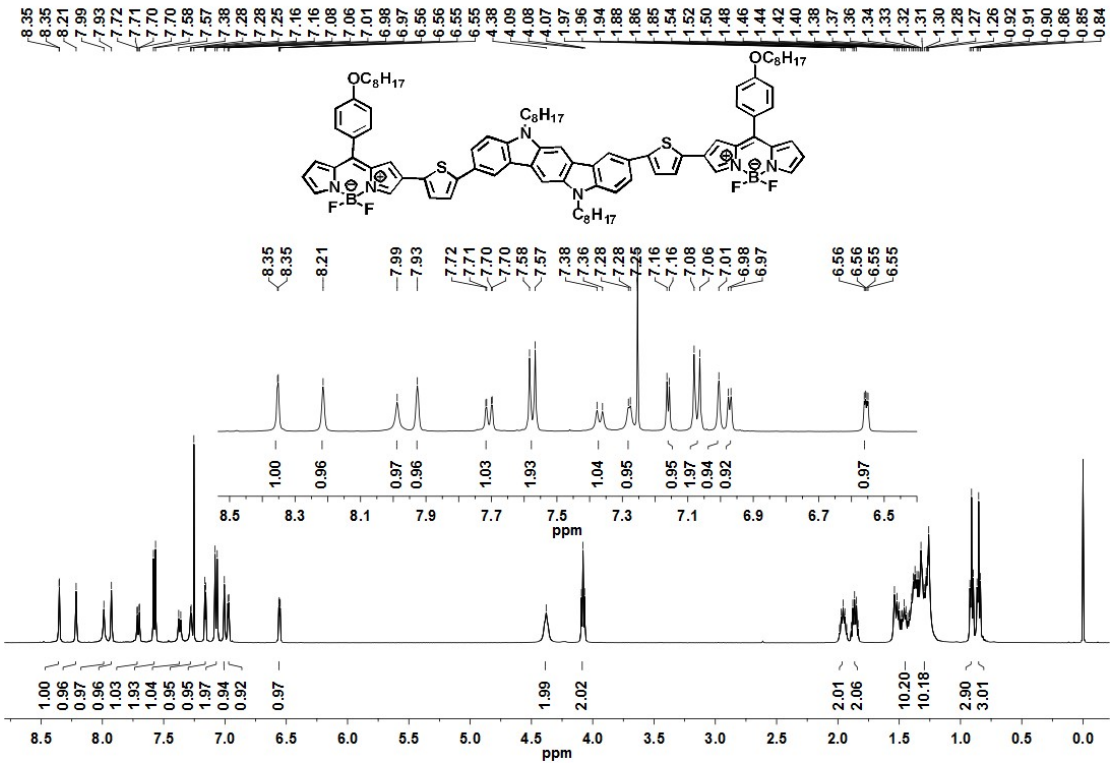

Fig. S9 ^{1}H NMR spectrum of **DCTBDP**

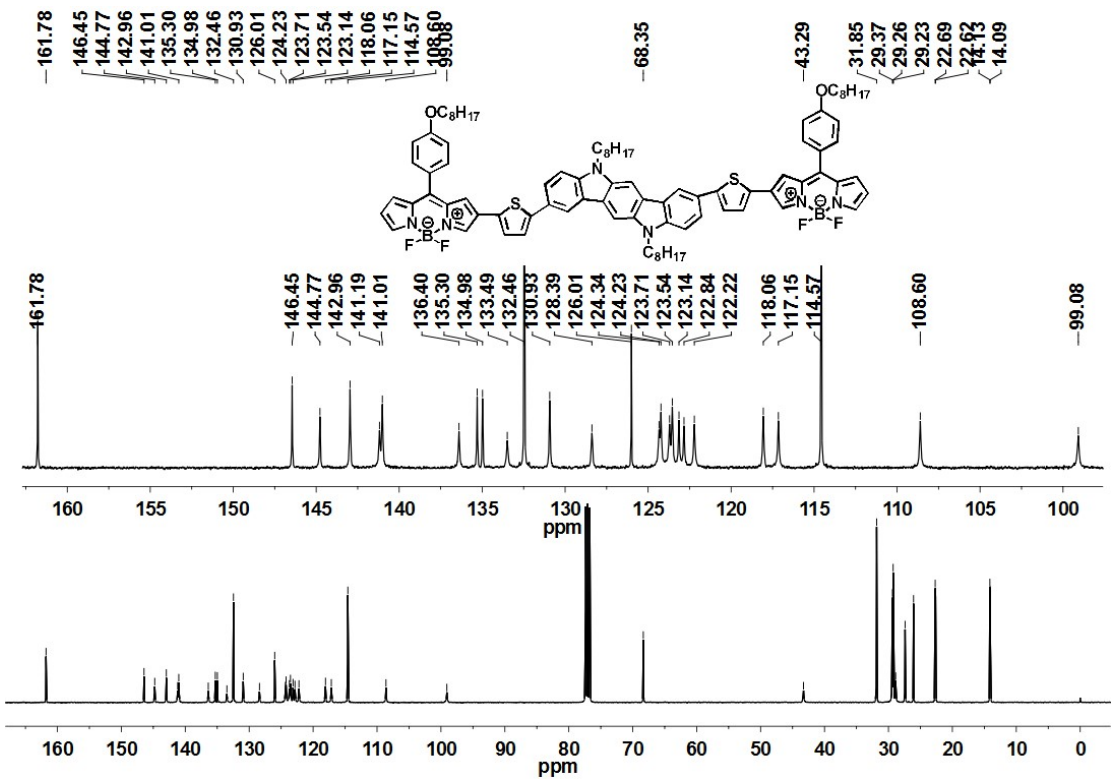

Fig. S10 ^{13}C NMR spectrum of **DCTBDP**

3. Photovoltaic device fabrication

The BHJ-OSCs were fabricated with a conventional device structure of ITO/PEDOT:PSS/SMDs:$PC_{71}BM$/Al. The indium tin oxide (ITO) coated glass substrates (10 Ω sq^{-1}) were cleaned with deionized water, methanol, acetone, toluene and iso-propyl alcohol, successively. Then poly(3,4-ethylenedioxythiophene):poly(styrene sulfonate) (PEDOT:PSS) as hole-transporting layer was spin-coated on the pre-cleaned ITO glass substrates at 4000 rpm for 60 s. Subsequently, the substrates were baked at 140 °C for 20 min in air and transferred to a N_2-filled glove box. The solutions of **CTBDP** or **DCTBDP**:$PC_{71}BM$ (1:2, w/w) at total concentration 12 mg mL^{-1} in chlorobenzene were stirred overnight at room temperature in N_2-filled glove box, and then D/A blend solutions were spin-casted on the top of PEDOT:PSS layer at 800 rpm for 60 s. Next, the blend films were dried at 100 °C for 5 min so as to remove residual organic solvent, and the prepared samples were exposed or not to CH_2Cl_2 vapor atmosphere at different duration. Finally, an aluminum (Al) cathode was deposited by vacuum thermal evaporation (*ca*. 10^{-4} Pa) through a shadow mask, yielding eight individual OSCs with 5.0 mm^2 effective area. Hole-only and electron-only OSCs were fabricated with the same process, apart from gold (Au) as cathode and zinc oxide (ZnO) as electron buffer layer, respectively. As for ZnO layer fabrication, a dispersive solution of ZnO nanoparticles in iso-propyl alcohol (Aladdin reagent) was spun-cast on the top of ITO substrates at 3000 rpm for 60 s, and then were annealing at 165 °C for 1 h in air.

4. Photovoltaic data

Table S3 PV data of the OSCs based on **CTBDP** and **DCTBDP**/$PC_{71}BM$ films under different conditions.

Donor	J_{SC} (mA cm^{-2})	V_{OC} (V)	FF	PCE_{max}($PCE^{\#}_{ave.}$) (%)
CTBDP	11.33	0.91	0.29	3.02(2.59)[a]
	15.69	0.81	0.41	5.26(5.02)[b]
	17.70	**0.81**	**0.41**	**5.85(5.28)**[c]
	14.90	0.81	0.43	5.22(4.31)[d]
DCTBDP	12.88	0.80	0.31	3.24(2.80)[a]
	14.59	**0.75**	**0.35**	**3.85(3.57)**[b]
	13.43	0.74	0.37	3.66(3.24)[c]
	11.74	0.55	0.37	2.39(2.02)[d]

[#] The average PCE is obtained from eight devices and all active-layer films are spin-casted from chlorobenzene solution (D/A=1:2, 12 mg/mL). For active layers: a----as-casted; b-d----CH_2Cl_2 vapor treatment for 30, 45 and 60 s respectively.

5. UV-vis absorption spectra of blend films

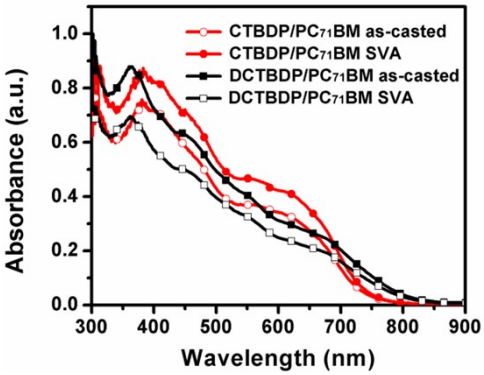

Fig. S11 UV-vis absorption spectra of **CTBDP** and **DCTBDP**/$PC_{71}BM$ blend films (w/w, 1:2) under different conditions.

6. Study of charge recombination

The charge recombination in **CTBDP** and **DCTBDP**-based devices were further investigated by the dependence of J_{sc} and V_{oc} with light intensity (P_{in}) (see **Fig. S12**). In general, the relationship between J_{sc} and P_{in} can be described as the power law: [2]

$$J_{sc} \propto (P_{in})^{\alpha}$$

in which α is the power exponent and represents the degree of bimolecular recombination in OSCs. The large a value from $\lg J_{sc}$ *versus* $\lg P_{in}$ curve means that bimolecular recombination process in OSCs at short circuit condition can be strongly suppressed. As shown in **Fig. S12(a)**, less bimolecular recombination was observed for the optimized **CTBDP** and **DCTBDP**-devices with slightly large α values of 0.923 and 0.921, respectively in comparison with the as-casted counterparts.

Under the condition of only bimolecular combination, the V_{oc} of a solar cell is primarily determined by the following equation: [3]

$$V_{oc} = \frac{E_{gap}}{q} - \frac{kT}{q}\ln\left(\frac{(1-P_D)\gamma N_c^2}{P_D G}\right)$$

where E_{gap} is the energy downshift between LUMO of the acceptor material and HOMO of the donor material; T is Kelvin temperature; k is Boltzmann constant; G refers to the generation rate of electron-hole pairs; P_D is the dissociation probability of electron-hole pairs; γ is the Langevin recombination constant and N_c is defined as effective density of states. Among them, P_D and N_c are independent of P while G is positively related to it. In principle, if bimolecular recombination is unique loss mechanism, the slope (S) of V_{oc} *versus* $\ln P_{in}$ curve should be equal to unity kT/q. However, when Shockley-Read-Hall (SRH) recombination (namely trap-assisted recombination) is involved, the S value remains the range of $1kT/q \sim 2kT/q$. If S value is very close to $2kT/q$, the recombination mechanism would be dominated by monomolecular recombination. As shown in **Fig. S12(b)**, the optimized OSCs especially for **CTBDP**-device exhibit the significantly suppressed trap-assisted recombination with smaller S value of $1.17kT/q$ among all OSCs, and therefore displaying better photovoltaic performance.

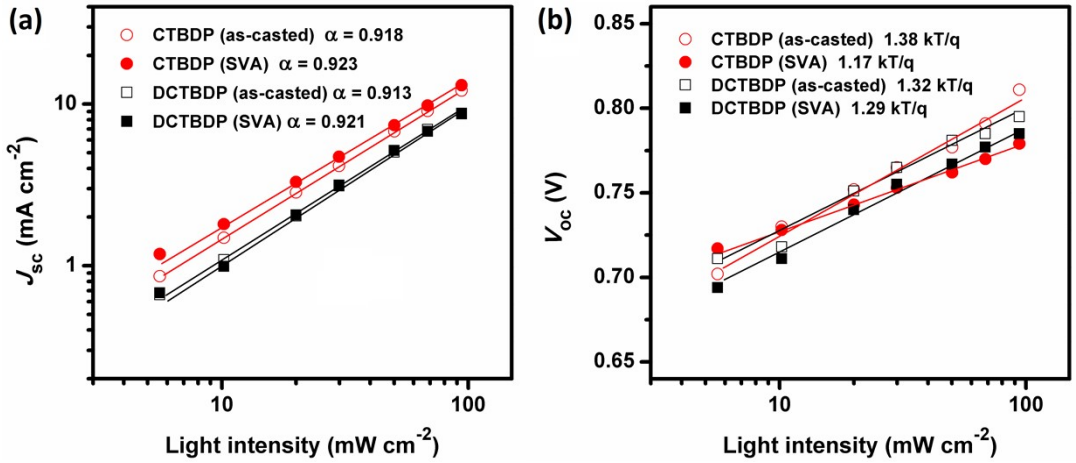

Fig. S12 Variation of **(a)** J_{sc} and **(b)** V_{oc} with the light intensity (5.6-94 mW cm^{-2}) for OSCs based on **CTBDP** and **DCTBDP**/$PC_{71}BM$ blend films under different conditions.

7. References

1. M. J. Frisch, G. W. Trucks, H. B. Schlegel, G. E. Scuseria, M. A. Robb, J. R. Cheeseman, G. Scalmani, V. Barone, B. Mennucci, G. A. Petersson, H. Nakatsuji, M. Caricato, X. Li, H. P. Hratchian, A. F. Izmaylov, J. Bloino, G. Zheng, J. L. Sonnenberg, M. Hada, M. Ehara, K. Toyota, R. Fukuda, J. Hasegawa, M. Ishida, T. Nakajima, Y. Honda, O. Kitao, H. Nakai, T. Vreven, J. A. Montgomery, Jr., J. E. Peralta, F. Ogliaro, M. Bearpark, J. J. Heyd, E. Brothers, K. N. Kudin, V. N. Staroverov, R. Kobayashi, J. Normand, K. Raghavachari, A. Rendell, J. C. Burant, S. S. Iyengar, J. Tomasi, M. Cossi, N. Rega, J. M. Millam, M. Klene, J. E. Knox, J. B. Cross, V. Bakken, C. Adamo, J. Jaramillo, R. Gomperts, R. E. Stratmann, O. Yazyev, A. J. Austin, R. Cammi, C. Pomelli, J. W. Ochterski, R. L. Martin, K. Morokuma, V. G. Zakrzewski, G. A. Voth, P. Salvador, J. J. Dannenberg, S. Dapprich, A. D. Daniels, O. Farkas, J. B. Foresman, J. V. Ortiz, J. Cioslowski, and D. J. Fox, Gaussian, Inc., Wallingford CT, 2009.

2. (a) F. Liu, H. Fan, Z. Zhang and X. Zhu, *ACS Appl. Mater. Interfaces*, 2016, **8**, 3661-3668; (b) L. Tanguy, P. Malhotra, S. P. Singh, G. Brisard, G. D. Sharma and P. D. Harvey, *ACS Appl. Mater. Interfaces*, 2019, **11**, 28078-28087.

3. W. Gao, M. Zhang, Z. Chen, X. Liu, K. Zheng, C. Zhong, F. Zhang and C. Yang, *J. Mater. Chem. C*, 2019, **7**, 10111-10118.